



Implementation and Performance Analysis of Single User-MIMO Test bed for Pilot Symbol Based TD-LTE Downlink Channels

Saeid Aghaeinezhadfirouzja, Hui Liu, Bin XIA

Department of Electronics Engineering, Shanghai Jiao Tong University, Shanghai, P.R.China.

ABSTRACT: This paper, design and utilize the implementation of 8×2 outdoor single-user multiple-input, multiple-output (SU- MIMO) systems for time division duplex TDD-LTE channels at 2.680 GHz to 2.690 GHz. With this purpose, there is a need for accurate and actual radio propagation model at these bands where around the Shanghai Jiao Tong University (SJTU) campus network. We develop a transformative test bed evaluation single user for real time network. In that SU-MIMO test bed, both the transmitter and the receiver communications are made by employing eight (four pairs of cross polarization) antennas in the transmitter side and 2 at the receiver for real time network. Measurements and challenges are to show the characteristics of the current physical downlink control channel (PDCCH) and physical downlink shared channel (PDSCH) sensitive to absolute power levels may not be enough to support a large number of UEs in a cell. Another weakness of the current cellular network is to reach an accurate synchronization such as coarse timing synchronization (CTS) between the received symbols. This CTS defect can lead to the severe performance degradation and issue for MIMO wireless systems.

KEYWORDS: Coarse Timing Synchronization (CTS), LTE, SU- MIMO, TDD (time division duplex), 2D Weiner filtering.

I.INTRODUCTION

Due to the increasing demand for multimedia data transmission in wireless mobile systems, there is an evident need for increasing the spectral efficiency of cellular systems. With their high spectral efficiency, SU-MIMO systems appear to be a crucial and fundamental part of future cellular systems. SU-MIMO provides significant benefits in wireless data rate and reliability of the link with a large number of antennas (more than 128) at the base-station (BS) [1]. Recently, network technology based on LTE advanced requires pilot overhead proportional to the number of antennas, based on this requirements with the increase of users we will have problem on OFDM sensitively. We use an experimentally recorded data set to compare the performance of sparse and conventional channel estimators under varying pilot overhead. We find that when increasing the pilot overhead at the cost of reduced data rate the performance saturates at some point.

In order to validate the theory, channel measurements must be carried on into test beds and actual applications. Using campus technological resources, prototypes were developed to determine the feasibility and commercial viability of SU- MIMO at campus network. Campus network made a huge outdoor SU-MIMO test bed then the performance of its practicality was evaluated after. The system is a channel processing that is used in measuring the wireless channel with a [2] large number of antennas to validate theoretical gains. 10 MHz bandwidths for channel measurements were taken over slow continuous user movements and also static-based users with different locations and then processed offline.

Pilot-based channel measurements were collected for both line of sight (LOS) and Non-line-of-sight (NLOS) environments. Issues to be addressed in most of the current cellular network are the theories and simulation works that lack of experimental supports [3] [4]. Our experimental research is designed to verify the theoretical results and model the effect of the SU-MIMO in a real-propagation environment. We have developed an extensive platform with four pairs of cross polarized antenna elements at the transmitter and 1 commercial Software-defined radio platform national instrument-universal software radio peripheral (NI-USRP2943R) with multiple antennas equipped with fully alignment, making it easy to access and modify. There are 5 different locations in a cell at different times. We propose a method to characterize different scenarios for active USRP and the achievable signals with LOS, NLOS environments by comparing the relationships of the different locations. We show that the angular power spectrum and I/Q performance at the base station results from a LOS and NLOS scenario when the user is at condition A, B, C, D and E both in static and dynamic positions respectively. It also shows how symbol conditions change as the user moves around the coverage area.

International Journal of Advanced Research in Electrical, Electronics and Instrumentation Engineering

(An ISO 3297: 2007 Certified Organization)

Vol. 5, Issue 4, April 2016

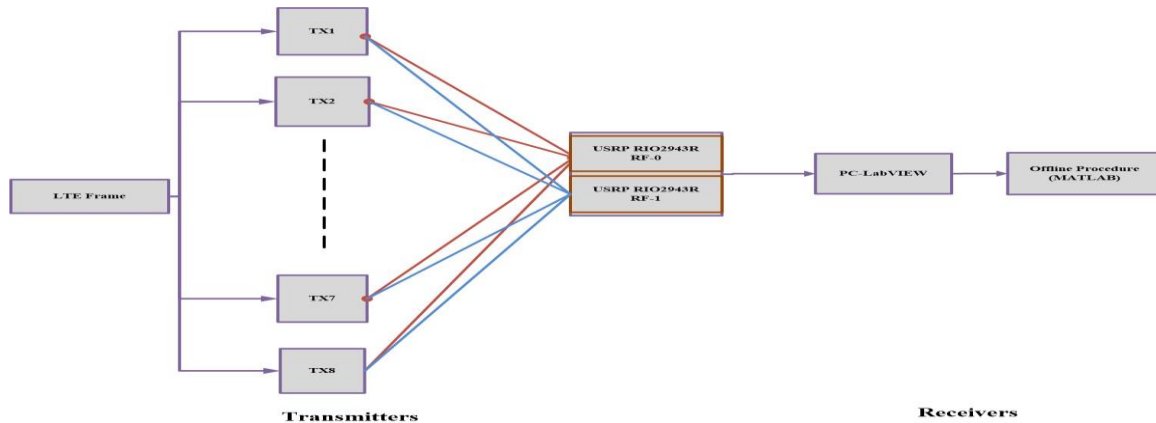


Figure 1: Block Diagram of SU-MIMO System.

1.1. Major contributions: Of our work include the implementation of a real-time radio test bed for multiple-antenna wideband system and the design of intrinsic waveform based on the test bed and the USRP is equipped with multiple antennas.

1.2. The main technical contributions: It include

- Developing achievable schemes for SU-MIMO-NI-USRP focused on data transmission over continuous-time and dispersive SU-MIMO channels where the transmitter knows all channels
- Showing the characteristics of the pilot symbol based detection and limitation of physical downlink channel for current cellular network
- Accurate CTS synchronization achieved between symbols respected to the pilot patterns.

1.3. Future contribution: the availability of field test SU- MIMO channel measurement data is critical to the verifications and the design of Massive MU-MIMO algorithms because all these algorithms rely on specific spatial and temporal structure of the underlying MU-MIMO channels.

1.4. The main objectives of this test bed are :

- Implementation of BS architectures to see the high throughput / low-latency processing requirements.
- CTS Synchronization procedure
- Formulation of 2D Weiner channel estimation.
- Aiming at the practical performance of current LTE frame structure.

II. SIGNAL MODEL

It considers a network recently, a worldwide convergence has occurred for the use of Orthogonal Frequency Division Multiplexing (OFDM) as an emerging technology for high-speed data transmission. OFDM uses a large number of narrow sub-carriers for multi-carrier transmission to carry data.

The block diagram of an OFDM transceiver is shown in Figure 2. Here, Information bits are grouped and mapped using Multiple Phase Shift Keying (MPSK) or Quadrature Amplitude Modulation (QAM) or Quadrature Phase Shift Keying (QPSK). Because an OFDM symbol is consists of a sum of subcarriers, the $n - thN \times 1$ mapped signal symbol χ_n is fed into the modulator using the Inverse Fast Fourier Transform (IFFT). Then, the modulated signal χ_n can be written as:

$$x_n = \frac{1}{N} \sum_{k=0}^{N-1} X_k e^{j2\pi kn/N}, n = 0, 1, \dots, N - 1, \quad (1)$$

Where N is the number of subcarriers or the IFFT size, k is the subcarrier index, n is the time index, and $1/N$ is the normalized frequency separation of the subcarriers. Note that χ_n and X_k form an N -point Discrete Fourier Transform (DFT) pair. The relationship can be expressed as:

$$x_n = DFT_N \{x_n\} \frac{1}{N} \sum_{k=0}^{N-1} X_k e^{j2\pi kn/N}, n = 0, 1, \dots, N - 1, \quad (2)$$

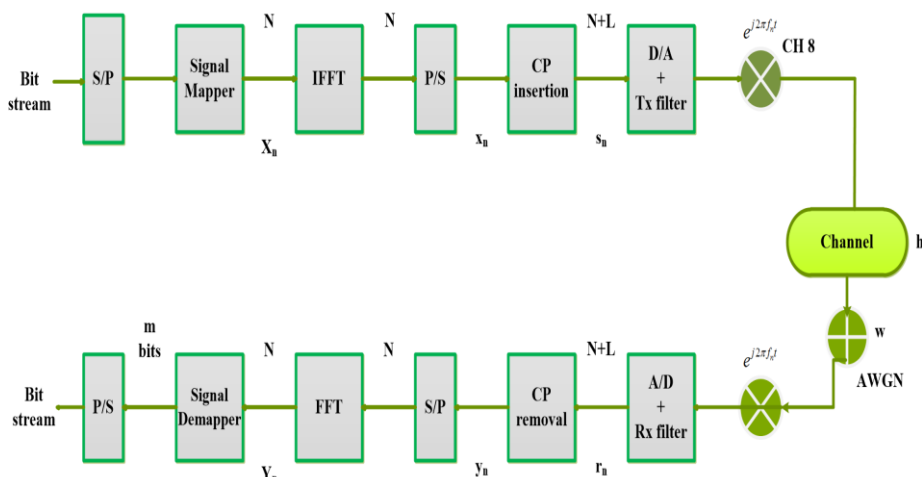


Figure 2: Block diagram of an OFDM transceiver.



Figure 3: Schematic Diagram of Experimental.

III. SYSTEM IMPLEMENTATION

The block diagram of SU-MIMO is shown in Figure.1. We used the available commercial base station to generate the LTE frame. The BS is mounted at the rooftop of the Biomedicine building of SJTU campus as shown in Figures.3 and 4. Channel measurement and waveform data processing at a baseband unit is processed at USRP. The central control PC is connected to each USRP unit via the GB ETHERNET port to control the procedures of the experiment including the time to start and end the measurement, parameters configuration etc.

3.1. Software Platform with Lab VIEW System Design: On the software side, the Lab VIEW development system provides an easy yet powerful interface to the USRP hardware allowing the rapid prototype of communication algorithms over the air. The NI-USRP software driver provides great functions. Lab VIEW can implement a high performance platform that is highly readable and customizable.

International Journal of Advanced Research in Electrical, Electronics and Instrumentation Engineering

(An ISO 3297: 2007 Certified Organization)

Vol. 5, Issue 4, April 2016

(2) The SU-MIMO Application framework uses Lab VIEW for its high productivity and ability to program and control the details of the I/O via Lab VIEW-(Field-Programmable Gate Array) FPGA. The acquired I/Q samples can be used to demodulate different types of analog modulated signals.

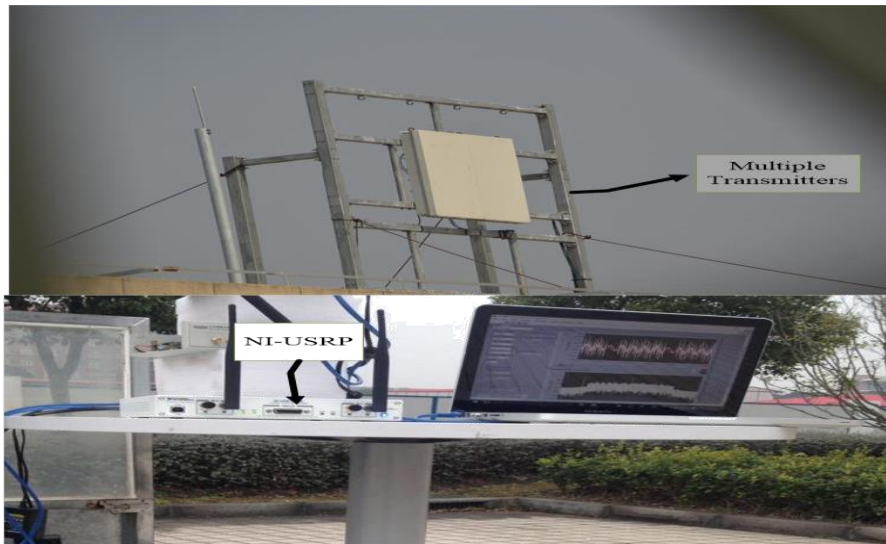


Figure 4: SU-MIMO centralized transmitter with multiple antennas.

In order to meet the Nyquist criterion, sampling rate must be done at least 20 Mbps with 10MHz bandwidth. The USRP efficiently meets this requirement and the USRP acts as a host in a local network, and the communication with the computer is done over IP address. The interface is done directly with Lab VIEW, which provides a set of modules required to work with this equipment configuring and establishing a connection, data acquisition and transmission, etc. Once a connection is set up, the USRP sends the sampled data at the request of Lab VIEW.

IV. SYNCHRONIZATION

In the downlink of our TD-LTE system, the receiver data needs to be synchronized with the LTE base station in the time and frequency domains to demodulate and to decode the desired data. The mechanism and process of synchronization is complicated that we are not going to elaborate it in detailed analysis due to the limitation of the space in the article. Here, we look briefly at coarse timing synchronization.

4.1. Coarse timing synchronization: CTS is the first step of our synchronization and the basis of the following steps. The purpose of the coarse timing is to locate arbitrary OFDM symbol among a LTE frame, to recognize the CP length and to estimate and compensate the fractional carrier frequency offset [5].

This paper employs joint maximum likelihood (ML) symbol time and carrier frequency estimator in OFDM systems [6] in CTS synchronization. The reason for this choice is its reliability and functionality in the initial search for OFDM symbol start as well as carrier frequency offset computation. The estimator marked as (; ") applied can be expressed as below:

$$\Lambda(\theta, \varepsilon) = |\gamma(\theta)| \cos(2\pi\varepsilon + \arg(\gamma(\theta))) - \rho\Phi(\theta) \quad (3)$$

Where

$$\gamma(\theta) \equiv \sum_{k=\theta}^{\theta+L-1} r(k)r^*(k + N_{DFT}) \quad (4)$$

and

International Journal of Advanced Research in Electrical, Electronics and Instrumentation Engineering

(An ISO 3297: 2007 Certified Organization)

Vol. 5, Issue 4, April 2016

$$\Phi(\theta) \equiv \frac{1}{2} \sum_{k=\theta}^{\theta+L-1} \left[|r(k)|^2 + |r(k + N_{DFT})|^2 \right] \quad (5)$$

Where L is defined here as the length of normal cyclic prefix NCP 1;2 in LTE specifications. By maximizing the estimator function, a which marks the start of an OFDM symbol in the recorded data can be found [7]. We use different cyclic prefix (CP) lengths for coarse time synchronization. Figure 5 shows the search window slides from the very beginning of the received sequence, and then we compare the first part and the last part inside the window. If these two parts are the same as down-sampling duration with CP length from $(1024 + CP) = 8$, we conclude that we have found a symbol. The received signal is combined with noise, but the error should be shorter than dedicated symbols duration.

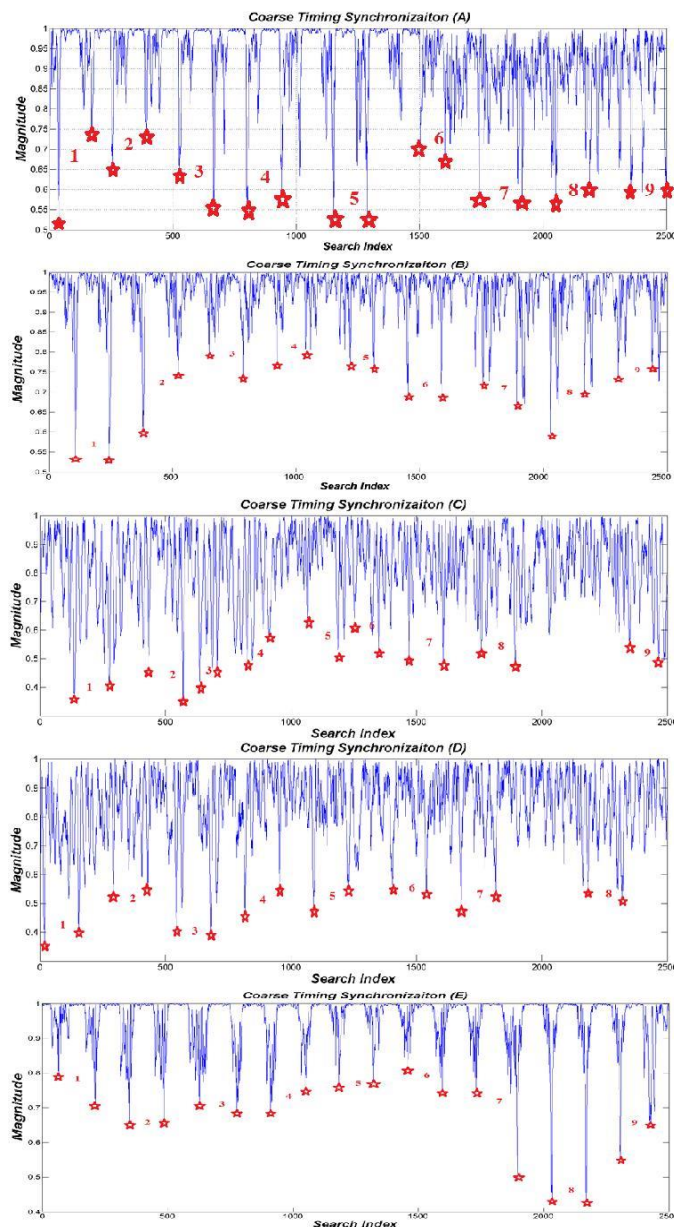


Figure 5: Coarse timing synchronization with NIFFT = 1024.

International Journal of Advanced Research in Electrical, Electronics and Instrumentation Engineering

(An ISO 3297: 2007 Certified Organization)

Vol. 5, Issue 4, April 2016

V. CHANNEL ESTIMATION PROCEDURE

This work adopts the time-frequency 2D Wiener filter channel estimation method in time domain based on the discrete distribution pilot of the downlink channel LTE system. In 2D channel estimation, the pilots are inserted in both the time and frequency domains, and the estimators are based on 2D filters with two concatenates a) 1D linear interpolations on frequency and b) time sequentially minimizes the system complexity. Channel response can be obtained using Wiener filter channel estimation method in both the frequency and time domains. The pilot pattern was based on LTE specifications where pilots were placed in a well-defined way to cover up the frequency and time domains [8] [9].

As Figure 6 shows a slot to show the structure of a resource block (RB), including PDCCH in LTE carries UE-specific scheduling assignments for Downlink (DL) resource allocation, PDSCH is the channel that carries all user data and all signaling messages and reference signals (RS). The location of the pilots and Physical downlink channel for 8 2 SU-MIMO transmission scheme in LTE specification.

5.1. LMMSE algorithms for channel estimation: In signal processing, a linear minimum mean square error (LMMSE) estimator is an estimation method which minimizes the mean square error (MSE) of the fitted values of a dependent variable.

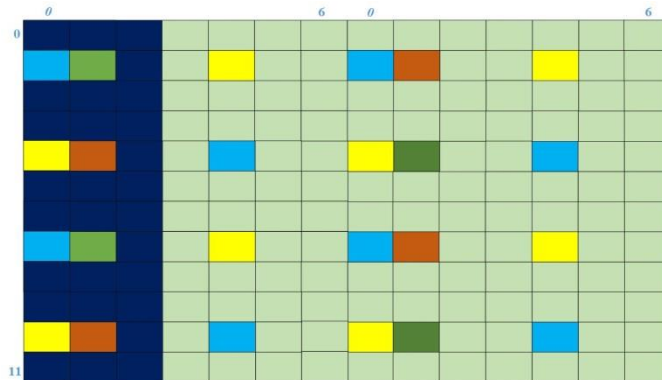


Figure 6: TD-LTE frame structure and resource block architecture.

IV. SECURITY

The mathematical representation for LMMSE [10] estimator of the channel frequency response in frequency. From LMMSE function, we are able to see that for LMMSE channel estimation algorithm requires frequency correlations.

5.2. Joint Time-Frequency Two-dimensional IWF Channel Estimation

The Wiener filter technique was applied in frequency for the OFDM symbols containing reference signals at the first stage of this technique. In the next step IWF was applied in time domain for all subcarriers within multiple OFDM symbols respectively [11]. The section is described as follows:

- IWF in Frequency Dimension: In this step, all reference signals in the same OFDM symbol between all subcarriers were used for channel frequency response.
- IWF in Time Dimension: Suppose that the estimated channel frequency responses after the first IWF in the Frequency domain of the n th subcarriers can be given as:

$$\hat{H}_{F,LMMSE}^{(n)} = \left[\hat{H}_0^{(n)} + \hat{W}_0^{(n)}, \dots, \hat{H}_i^{(n)} + \hat{W}_i^{(n)}, \dots, \hat{H}_{L-1}^{(n)} + \hat{W}_{L-1}^{(n)} \right]^T \quad (6)$$

Where L is the number of the OFDM symbols with reference signals within each sub-frame. $\hat{H}_i^{(n)}$ and $\hat{W}_i^{(n)}$ are the channel frequency response and the corresponding residual noise of the n th subcarrier in the i th OFDM symbol with reference signals. After IWF based on LMMSE algorithm in the time domain for the n th subcarrier to reduce the corresponding residual noise, yields [8].

VI. SYSTEMS ANALYSIS

Measurements made in the lab and extensive field trials show that LTE performs well in the physical layer. Multi-stream SU-MIMO yields good gains in realistic environments, improving peak rates [12]. We extract frame from the

International Journal of Advanced Research in Electrical, Electronics and Instrumentation Engineering

(An ISO 3297: 2007 Certified Organization)

Vol. 5, Issue 4, April 2016

measured data and investigate the frame (symbols) behaviour of SU-MIMO. Systems analysis, scenario analysis ,data processing system and observed frame behaviour are presented in the following parts.

6.1. Scenario Analysis:

The designated area to capture signal is around the Biomedicine building since the antennas are mounted on the rooftop of the Biomedicine department building.

The results of the frame transmission and subsequent analysis in dependence on the SNR for all antenna configurations and models of transceiver location used are listed in this section. Five areas were selected as static and dynamic locations for capturing signals with LOS and NLOS environments, as shown in Figure 3. The locations are in a triangle formation with each one having a certainly specific received power and the gain of the antenna. The first location (A) LOS is set very close to the BS, the second (B) LOS, the third (C) NLOS and the fourth (D) NLOS locations are set at 50, 500, 650 and 700 meters respectively. For the dynamic (E) aspect, locations were set to be moving in a circle formation from the original positions at the speed of 15 km/hr.

The base station height was about 50 meter from the ground, the USRP reception antenna height in all locations were 2 meters with the frequency range of 2.680 2.690 GHz. The NI-USRP is able to sample the signal and acquire I/Q (In-Phase and Quadrature) data with a rate of 20 Mega-samples/sec and send them via Ethernet cable to be processed with NI-Lab VIEW in the central PC. As we can see in Figure 7, the result is based on power spectrum and IQ graph which came out from different scenarios where the user is located in the campus.

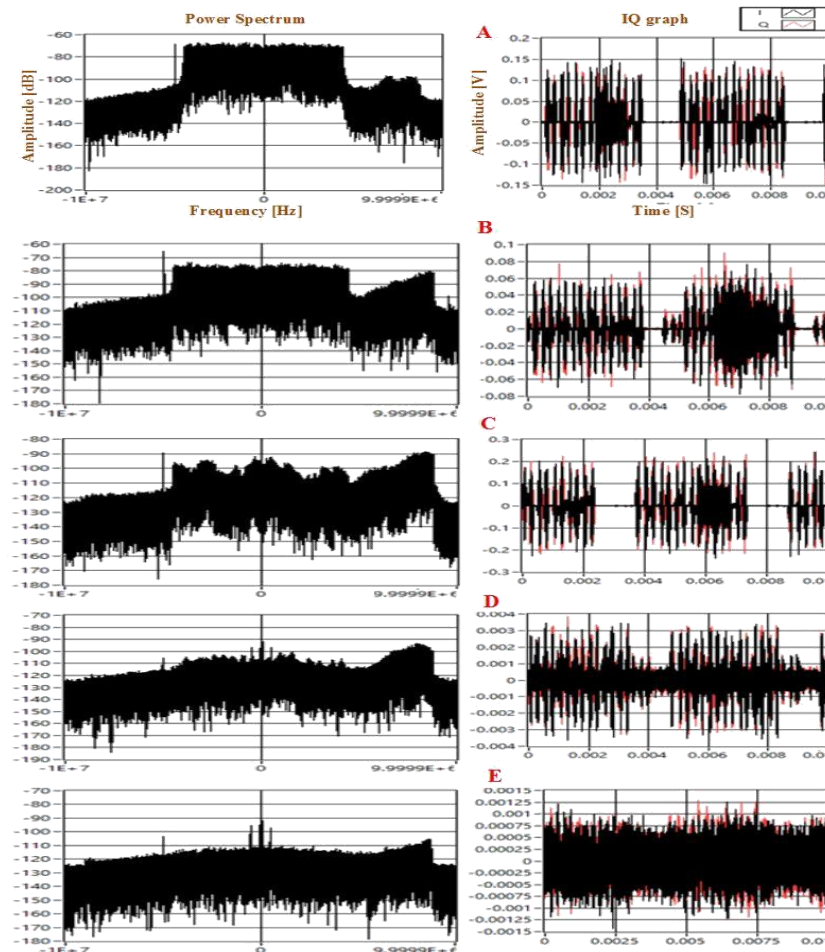


Figure 7: Power spectrum and IQ graph both in static and dynamic locations.

International Journal of Advanced Research in Electrical, Electronics and Instrumentation Engineering

(An ISO 3297: 2007 Certified Organization)

Vol. 5, Issue 4, April 2016

Parameters	Values
Frequency range	2:680 (GHz) to 2:690 (GHz)
Duplexing	TDD
Channel Coding	TurboCode
Channel Bandwidth	10 (MHz)
FFT Size	1024
CP Length	80; 72Normal
Total Symbols	140s
Transmission Bandwidth Configuration	50RBs
Modulation Schemes	QPSK; QAM
Multiple Access Schemes	OFDM

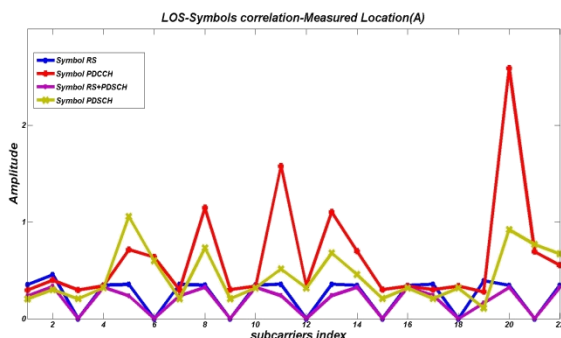
Table 1: Transceiver parameter settings.

6.2. Data Processing System

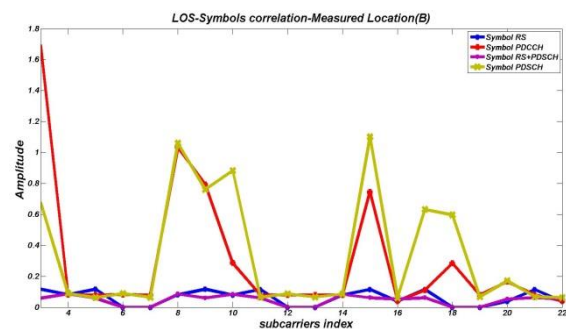
The measurements can be shown in Figures 8 (LOS), (NLOS) and 9 (Dynamic), based on this platform, we can test the performance of the algorithm; compare preponderance and meanness of different transmission scheme. In the following paragraph, simulation results were given to demonstrate the performance of the joint time-frequency two-dimensional estimator proposed for the 3GPP LTE downlink system. In relation to this, a SU-MIMO system based on the 10MHz LTE downlink physical layer parameters was considered.

An OFDM system with $K = 600$ sub-carriers, $N=140$ symbols were simulated, and cyclic prefix lengths $L = 80, 72$ with $N_T = 8$ transmitters and $N_R = 2$ receiver antennas were used. The frame structure is consisting of RS, PDCCH and PDSCH based on LTE specifications. In the current setting, the test bed operates with multiple parameters similar to LTE standards shown in Table I.

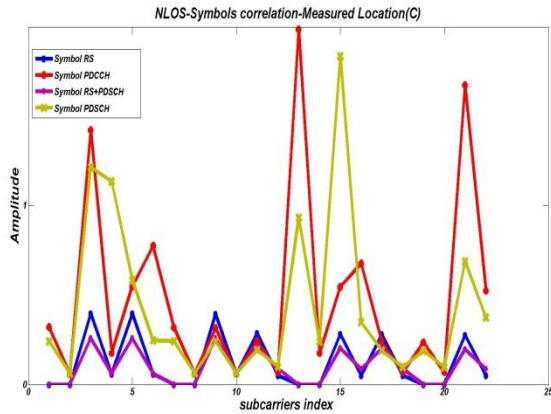
We analysis real symbols behave in different scenarios. We have performed simulations and the results are summarized in 5 cases. After H was estimated, one slot was selected to analyse frame conditions which carrying reference signals, PDCCH and PDSCH. Figures show that the symbol behaviour does not only vary depending on the scatter effect but also on the physical position of the symbol and the size of random stream undergoes physical channels coding to rate match the transport block to the available physical channel bits [10]. As can be seen from presented graphs, the amplitude of PDSCH and PDCCH are sensitive to absolute power levels in all cases because of the carrying data stream. This is given by the size of the data transmitted and modulation schemes used for different scenarios and the used channel coding. One can see from figures that the performance of existing LTE frame structure on PDCCH and PDSCH at higher symbol modulation orders are more sensitive to noise interference and thus will suffer degradation in performance when compared to lower symbol modulation orders schemes at similar SNR values. To solve this problem of power difference between two groups of symbols, we can put lesser power to the non-reference signal channels at the symbol carrying reference signal.



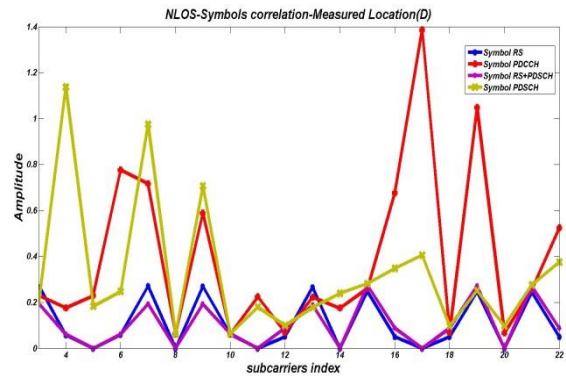
a) LOS, 50m far from BS. In this condition there is no cell interference and effective noises after 10 PM



(b) LOS, 500m far from the BS. In this part some scattered effects were on the received signals. They were captured after in the evening on a windy night



(c) NLOS on a sunny afternoon with a lot of noises from the environment, 650m from the BS. In this part, there are many trees and a huge building which also affected the received signals



(d) NLOS in the evening, 700m from the BS. In this part some scattered road noises affected the received signals

Figure 8: Different scenarios of frame behaviour

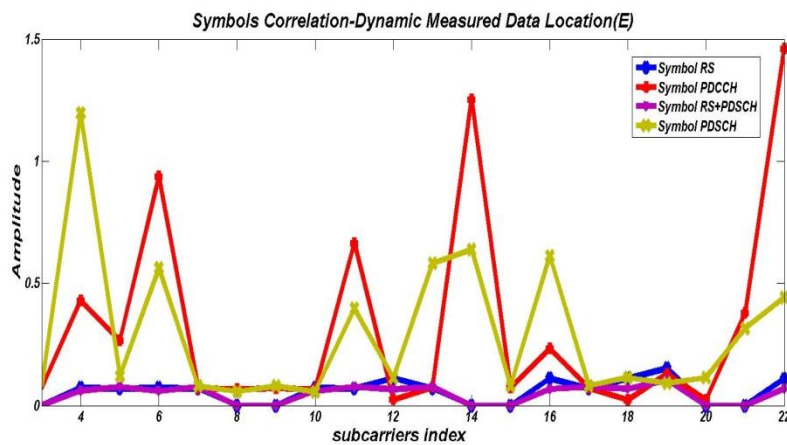


Figure 9: Dynamic, 50m to 1000m from the BS in a circular formation. In this part some scattered buildings and cars affected the received signals in the evening.

VII. CONCLUSION

This paper details our clearing to meet the TDD-SU-MIMO in a practical testing environment. The testbed operates at 10 MHz bandwidth. One USRP serves as a receiver and eight centralized antennas as transmitter. We have hierarchical architecture, hardware, bandwidth partitioning and a procedure of communication protocol that allows the meeting of real-time processing. With the knowledge of these fundamental parameters, the coarse timing synchronization of the recorded signals is performed using the cross-correlation property of the cyclic prefix in OFDM symbols. Based on the downlink LTE pilot channel system, this paper presents a time-frequency Wiener filter channel estimation algorithm provided by the IWF on LMMSE algorithm in both time and frequency do-mains. The LOS and the NLOS frame performance results show differences in the static and dynamic cases because of noises, carrying data and the bit stream size of physical channel. Finally, we have analysed power difference between the PDSCH transceiver signal processing procedure, PDCCH simulation platform and the performance of reference signals.



International Journal of Advanced Research in Electrical, Electronics and Instrumentation Engineering

(An ISO 3297: 2007 Certified Organization)

Vol. 5, Issue 4, April 2016

REFERENCES

1. P Hoehner, S Kaiser, et al. Two-dimensional pilot-symbol-aided channel estimation by wiener filtering, in Acoustics, Speech, and Signal Processing, 1997. ICASSP-97., 1997 IEEE International Conference on, IEEE, 1997; 3: 1845–1848.
2. J Zhu, H Li, On the performance of lte physical downlink shared channel, in Computer Science and Network Technology (ICCSNT), 2011 International Conference on, IEEE, 2011; 2: 983–986.
3. AR Varma, C Athaudage, et al. Optimal superimposed pilot selection for ofdm channel estimation,” in Signal Processing Advances in Wireless Communications, 2006. SPAWC’06. IEEE 7th Workshop on. IEEE, 2006; 1–5.
4. S Wu, CX Wang, et al. A non-stationary 3-d wideband twin-cluster model for 5g massive mimo channels, Selected Areas in Communications, IEEE Journal on, 2013; 32: 1207–1218.
5. A Golnari, M Shabany, et al. Design and implementation of time and frequency synchronization in lte, 2015.
6. JJ Van de Beek, M Sandell, et al. ML estimation of time and frequency offset in ofdm systems, IEEE transactions on signal processing, 1997; 45: 1800–1805.
7. S Lu, Channel characterization for lte, a thesis presented,” The Department of Electrical and Information Technology, 2013; 1–49.
8. J Hou, J Liu, A novel channel estimation algorithm for 3gpp lte downlink system using joint time-frequency two-dimensional iterative wiener filter, in Communication Technology (ICCT), 2010 12th IEEE International Conference on. IEEE, 2010; 289–292.
9. G Auer, Channel estimation in two dimensions for ofdm systems with multiple transmit antennas, in Global Telecommunications Conference, 2003. GLOBECOM’03. IEEE, 2003; 1: 322–326.
10. Y Shen, E Martinez, Channel estimation in ofdm systems, Application note, free scale semiconductor, 2006.
11. K Zhong, X Lei, et al. Wiener filter based channel estimation for high-speed communication environments, Wireless Personal Communications, 2013; 69: 1819–1845.
12. Y Song, N Guo, et al. Fpga based uwb mimo time-reversal system design and implementation,” in Ultra-Wideband (ICUWB), 2010 IEEE International Conference on, IEEE, 2010; 2: 1–4.